

# Discrete solitons in coupled active lasing cavities

Jaroslav E. Prilepsky,<sup>1,\*</sup> Alexey V. Yulin<sup>2</sup>, Magnus Johansson<sup>3</sup>, and Stanislav A. Derevyanko<sup>1</sup>

<sup>1</sup>*Nonlinearity and Complexity Research Group, Aston University, Aston Triangle, B4 7ET, Birmingham, UK*

<sup>2</sup>*Centro de Fisica Teorica e Computacional, Faculdade de Ciencias, Universidade de Lisboa, Lisboa 1649-003, Portugal*

<sup>3</sup>*Department of Physics, Chemistry and Biology (IFM), Linköping University, SE-581 83 Linköping, Sweden*

\*Corresponding author: y.prylepskiy1@aston.ac.uk

Compiled February 22, 2012

We examine the existence and stability of discrete spatial solitons in coupled nonlinear lasing cavities (waveguide resonators), addressing the case of active media, where the gain exceeds damping in the linear limit. A zoo of stable localized structures is found and classified: these are bright and grey cavity solitons with different symmetry. It is shown that several new types of solitons with a nontrivial intensity distribution pattern can emerge in the coupled cavities due to the stability of a periodic extended state. The latter can be stable even when a bistability of homogenous states is absent. © 2012 Optical Society of America

OCIS codes: 190.1450, 190.4390, 190.4420

Cavity solitons have attracted appreciable attention as their stability and high robustness make them excellent candidates for multipass optical delay lines, spatial information encoding, and manipulation/reconfiguration based on the transverse distribution of light [1,2]. These objects represent a particular realization of the dissipative soliton notion – localized solutions of nonlinear equations existing due to the balance between attenuation, gain, nonlinearity and diffraction [2]. Recently there has arisen a significant interest in studying discrete cavity solitons (DCS) [3–8], which are localized excitations in coupled arrays of nonlinear cavities. Notably, the existence and stability properties of DCS can be essentially different from those of the continuous counterparts, and moreover, the continuum limit of such solutions can be absent at all [3–5]. At the same time the self-organization and emergence of localized structures in lasing cavities are also the subjects of intensive theoretical [2,8] and experimental [9,10] study. The important difference of lasing systems is that there one can have solitary solutions maintained by a simultaneous balance between both linear and saturable gain/loss impact [2,6,8]. In this Letter we consider DCS in the system of coupled lasing cavities, taking into account linear loss, Kerr nonlinearity and gain saturation. For the first time to our knowledge, we address the localized excitations in discrete *active* systems, where in a low amplitude regime the gain term dominates over the attenuation. In this Letter we show that, due to the presence of external driving, this system can support versatile families of stable localized solutions unless the gain is bigger than a particular value. We also present a *new type of DCS*, which has not been studied so far in other discrete coupled-cavity systems.

We consider the array of waveguides and will use the model developed in [4] taking into account the interaction between the neighboring cavities only. Characterizing the field in each cavity by slow varying amplitude  $A_n$  we write down the resulting normalized equation for the

field amplitude inside the  $n$ -th optical resonator as:

$$\left( i \frac{d}{dt} + \Delta + i\delta + \alpha|A_n|^2 - \frac{i\gamma}{1 + |A_n|^2} \right) A_n + C(A_{n+1} + A_{n-1} - 2A_n) = P \cdot e^{i\kappa n}. \quad (1)$$

In Eq.(1)  $C$  characterizes the strength of coupling,  $\tilde{\Delta} = \Delta - 2C$  is the detuning of the pump frequency from the resonant one (we explicitly extracted the term  $2C$  to have a second difference); parameter  $\delta > 0$  describes the linear losses,  $P \geq 0$  is the amplitude of the driving field (normal incidence is considered,  $\kappa = 0$ ),  $\alpha$  characterizes the strength of the nonlinear (Kerr) polarization, and  $\gamma > 0$  is the lasing gain. We are engaged with the case of *active lasing media*, and thus inequality  $\gamma > \delta$  holds; this implies that in the absence of driving field ( $P = 0$ ) the trivial solution  $A_n = 0$  is modulationally unstable [8]. The field  $A_n$  is normalized to the lasing saturation intensity  $I_0$ :  $A_n/\sqrt{I_0} \rightarrow A_n$ ; the time  $t$  is also normalized by the cavity relaxation time (for the exact normalization in Eq.(1) see [4,7]). For presenting the results we opt for the following typical values of normalized input parameters:  $\Delta = 3.5$ ,  $\delta = 0.4$ ,  $\gamma = 1.7$ . Further we focus on the discrete solutions that do not have continuum counterparts [4,7], and deal with a weak *defocusing* nonlinearity:  $\alpha = -0.2$ . So, the solutions can exhibit sharp spatial changes with scales of the order of the inter-cavity separation. We use (unless otherwise stated) the relatively weak coupling strength  $C = 0.15$ . We notice that by applying the symmetry transformations [7] one can readily compose the counterparting solutions for other values of parameters starting from the families given below.

First we address the extended static states of Eq.(1). For the homogeneous (H) pattern, setting  $A_n = A$ , one finds the so-called response curve  $P(|A|)$ : it can have either one or three solutions depending on the system parameter values, and in the latter case one can have bistability between the low-intensity (H1) and high-intensity (H2) homogeneous states. The curve  $P(|A|)$  for the set

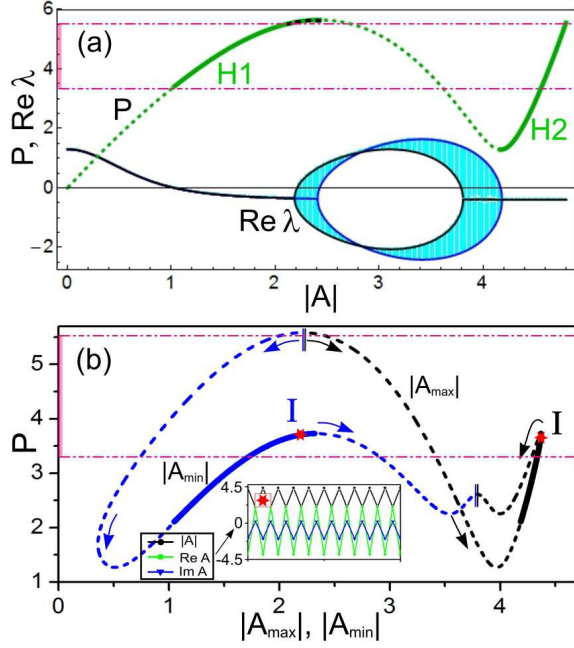


Fig. 1. (Color online.) Response curves for homogeneous and periodic solutions with stable regions marked by thick lines. Pane (a): The curve  $P(|A|)$  for the homogeneous H-solutions, with stable lower (H1) and higher (H2) states (the dash-marked top of H1 is also unstable for  $C > 0$ ); below this curve we show the spectrum of  $\text{Re}[\lambda]$  (shadowed region), the boundaries  $q = 0$  and  $q = \pi$  are drawn by solid lines. Pane (b): The curves  $P(|A_{\max}|)$  and  $P(|A_{\min}|)$  for the periodic inhomogeneous I-solution, the direction of ‘evolution’ from the curve coalescence points (marked by ||) is identified with arrows. The inset shows the I-solution profile corresponding to the point ‘\*’ on the snakes. The horizontal dash-dot lines and the highlighted parts on the  $P$ -axis indicate the bistability region for homogeneous solutions.

of parameters chosen is given in Fig.1(a) and it is multivalued for some diapason of  $P$ .

One can also find the *inhomogeneous periodic static solutions* of Eq.(1) (we label these as I-solutions), having a 2-site period: we set  $A_n, A_{n+2}, \text{etc.} = A_{\max}$ , and  $A_{n+1}, A_{n+3}, \text{etc.} = A_{\min}$ ,  $A_{\max} \neq A_{\min}$ , and then solve the system for these two complex fields. The results are given in Fig.1(b) in the form of two (equivalent) snaking response curves:  $P(|A_{\max}|)$  and  $P(|A_{\min}|)$ . The I-solutions are discrete and do not exist in the continuum limit. In general, infinitely many extended solutions with more complex spatial patterning can be found but here we restrict ourselves to these three simplest families.

We are aiming to study solitons forming on H or I backgrounds and so the stability of these states is of importance. To analyze the stability we linearize Eq.(1) and solve the eigenvalue problem for small excitation  $a_n(t) = a_{(1)}e^{\lambda t + iqn} + a_{(2)}e^{\lambda^* t - iqn}$  on the background  $A$ . The background is stable if  $\text{Re}[\lambda] \leq 0$  for all  $\lambda$ .

We see, Fig.1(a), that for the parameters chosen we

have a region of bistability (highlighted). Note, that the modulational instability of the part of H1-branch for low  $P$  and  $|A|$  values is a characteristic feature of active cavities, and is absent for passive case [4, 6, 7]: the stability region grows towards lower values of  $P$  as the ‘activeness’ of the medium diminishes, i.e. when  $\gamma$  tends to  $\delta$ . For any  $\delta$  there is a threshold value of gain,  $\gamma_{\max}(\delta, \Delta, \alpha)$ , where the the only stable H-state is the high-intensity one, H2.

The stable region of I-state corresponds to the highlighted snake parts in Fig.2(b). The stability regions of H1 and H2 partially overlap with that of the I-solution but the I-state can be stable when H1 is unstable, i.e. in the region where one does not have the bistability of H-states. We emphasize that this nonlinear extended I-state has not been studied before for the systems of coupled optical cavities [3, 4, 7], and its existence and stability allow composing *new stable DCS families*.

Static DCS can now be found in the form of (homoclinic) connections between the aforementioned three stable states: homogeneous ones H1 and H2, Fig.1(a), and a periodic inhomogeneous I-state, Fig.1(b). In Figs.2 and 3 we protocol our DCS found in the model Eq.(1), presenting these on the snaking diagrams: each point on a snake corresponds to a particular DCS. The DCS can be divided into two subclasses according to whether the intensity in the soliton center is higher (bright solitons, Fig.2) or lower (grey solitons, Fig.3) compared to the background [4, 7]. It is convenient to characterize the bright/grey DCS by the maximal/minimal amplitude of the soliton. The simplest DCS correspond to the connection between two homogeneous states: H1-H2-H1 for bright DCS, i.e. ‘humps’ of intensity residing on the H1 background (see Figs.2(a)-(c) and the profiles of stable solution at panes corresponding to the points ‘1’, ‘2’ and ‘3’), and H2-H1-H2 for grey DCS, i.e. an intensity ‘dent’ in the H2 background (not shown). Both these types of DCS can be stable in the active media described by Eq.(1), see the highlighted regions on the snaking curves in Figs.2(a)-(c) for the stable bright DCS. The solitons can exist only up to a finite value of coupling: in Fig.2(a) the  $C(|A_{\max}|)$  dependencies for bright DCS turn down after passing a maximum point, and the same situation holds for the grey solitons, i.e. these solutions do not exist in the continuum limit  $C \rightarrow \infty$ . The snaking diagram in terms of  $P(|A_{\max}|)$  for the H1-H2-H1 bright DCS is given in Fig.2(b), but since the stable winds of the  $P(|A_{\max}|)$ -snake are hardly distinguishable for this solitonic family, a more representative diagram can be plotted in terms of the solution mass,  $M = \sum_n |A_n - A_b|^2$ , with  $A_b$  being the background field value. On this plot [Fig.2(c)], the hierarchy with respect to the growth of the number of excited DCS sites is clearly seen.

The *new families* of DCS correspond to connections of the homogeneous states with the I-state: bright H1-I-H1, and grey H2-I-H2; see Figs.2(d), (e) and Fig.3, correspondingly, for the snaking diagrams in terms of  $P(|A_{\max}|)$ ,  $M(|A_{\max}|)$  and  $P(|A_{\min}|)$ . As one can see, these DCS have a nonuniform central excited part cor-

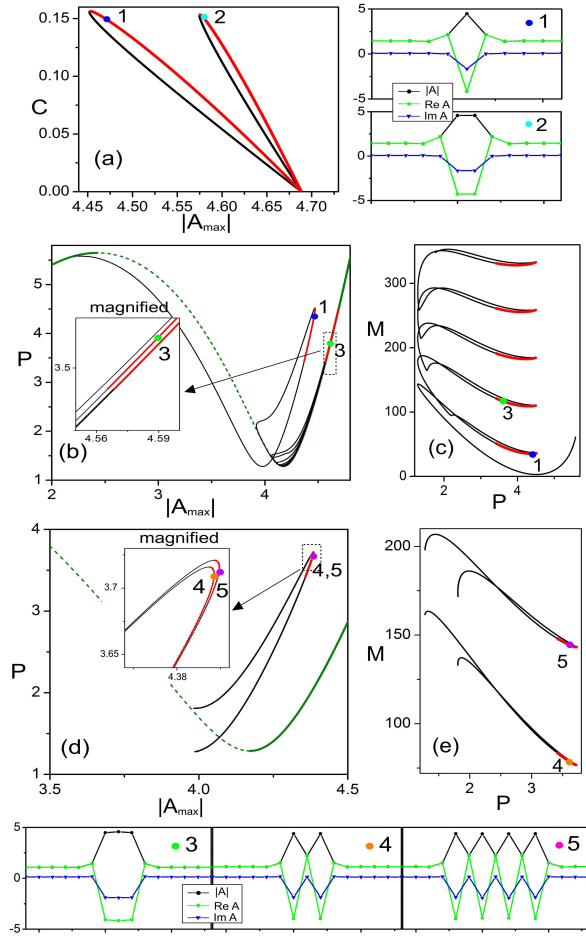


Fig. 2. (Color online.) Snaking diagrams (stable regions are highlighted) and solution profiles for bright DCS. (a) The curve  $C(|A_{\max}|)$  for fixed  $P = 4.47$  corresponding to the 1- and 2-site H1-H2-H1 solutions. Panes (b) and (c) are the diagrams for the site-centered H1-H2-H1 solutions in terms of  $P(|A_{\max}|)$  and  $M(|A_{\max}|)$ , panes (d) and (e) – the same for the H1-I-H1 solutions. The small panes right to panel (a) and below the figure show the particular stable distributions referring to the points on the snakes marked as • '1'–'5'.

responding to a fragment of the I-state embedded into either H1 or H2 background (see the profiles for points • '4', '5', and ■ '6'). These 'nontrivial' solitons are stable for some range of parameters, see the highlighted parts of the snakes. Note, that grey DCS of this type can be stable in the region, where solitons referring to the connections of the H-state are unstable, Fig.3. It is also possible to compose yet another new type of stable DCS in the form of a uniform H1 or H2 segment embedded into a periodic inhomogeneous I-background, due to the intersection of the stability regions for the H- and I-states.

To conclude, we have found a zoo of localized static solutions corresponding to stable DCS in coupled laser cavities; bright DCS are protocolled in Fig.2 and

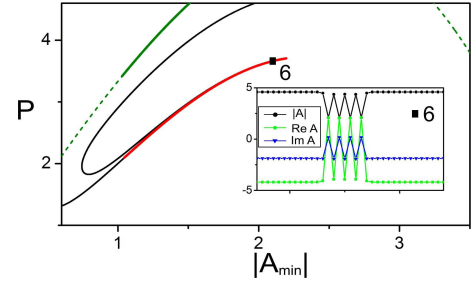


Fig. 3. (Color online.) Snaking diagram  $P(|A_{\min}|)$  for the grey DCS corresponding to the H2-I-H2 connection. The inset shows the particular distribution referring to the point marked as ■ '6'.

grey ones in Fig.3. Aside from 'conventional' DCS, corresponding to the connections between homogeneous states H1 and H2, we have found a new type of DCS involving a periodic inhomogeneous I-state, which has not been found before in optical cavities. The existence of the great variety of stable DCS paves the way to the more versatile and sophisticated patterning of transverse light distribution. At the same time our study poses an interesting question of whether the 'nontrivial' DCS, like those exemplified by solutions • '4', '5' and ■ '6', can be stable in other systems of coupled optical cavities, like a discrete Lugiato-Lefever model [4]. Notably, these solitons can be stable when the bistability of H-states is absent.

A.Y. and M.J. thank NCRG, Aston University, for kind hospitality. M.J. also acknowledges support from the Swedish Research Council. A.Y. was supported by the FCT (Portugal), grant PTDC/FIS/112624/2009.

## References

1. U. Peschel, D. Michaelis, and C. O. Weiss, IEEE J. Quantum Electron. **39**, 51 (2003).
2. "Dissipative Solitons: From Optics to Biology and Medicine," N. Akhmediev and A. Ankiewicz (Eds.), Series: Lecture Notes in Physics, Vol. 751, (Springer-Verlag: Berlin, Heidelberg), 2008.
3. F. Lederer, G.I. Stegeman, D.N. Christodoulides, G. Asanto, M. Segev, and Y. Silberberg, Phys. Rep. **463**, 1 (2008).
4. U. Peschel, O. Egorov, and F. Lederer, Opt. Lett. **29**, 1909 (2004).
5. O. Egorov, F. Lederer, and K. Staliunas, Opt. Lett. **32**, 2106 (2007).
6. A.V. Yulin, A.R. Champneys, and D.V. Skryabin, Phys. Rev. A **78**, 011804(R) (2008).
7. A.V. Yulin and A.R. Champneys, SIAM J. Appl. Dynam. Syst. **9**, 391 (2010). For the symmetry transformations see specifically Eqs.(2.8)-(2.10) of this Ref.
8. Al. S. Kiselev, An. S. Kiselev, and N. N. Rozanov, Opt. Spectrosc. **105**, 547 (2008).
9. P. Genevet, S. Barland, M. Giudici, and J.R. Tredicce, Phys. Rev. Lett. **101**, 123905 (2008).
10. Y. Tanguy, T. Ackemann, W. Firth, and R. Jäger, Phys. Rev. Lett. **100**, 013907 (2008).